

Simultaneous Information and Energy Transfer in Large-Scale FA-enabled Cellular Networks

Christodoulos Skouroumounis and Ioannis Krikidis

IRIDA Research Centre for Communication Technologies,

Department of Electrical and Computer Engineering, University of Cyprus, Cyprus

Email: {cskour03, krikidis}@ucy.ac.cy

Abstract—In this paper, we study the performance of fluid antenna (FA)-enabled user equipments (UEs) in the context of simultaneous wireless information and power transfer (SWIPT) networks. All UEs have successive interference cancellation (SIC) capabilities and employ a novel port selection (PS) scheme. In contrast to existing PS approaches, where the FA port with the highest signal-to-interference ratio (SIR) is selected, a UE communicates with its serving base station (BS) through the port that offers the minimum SIR. The proposed PS scheme leverages the additional degree of freedom offered by the FA technology to ensure the successful implementation of the SIC process, leading to an improved information decoding (ID) and energy harvest (EH) performance. By using stochastic geometry tools, analytical expressions for the ID and EH outage probability are derived. Our results illustrate that the employment of the proposed PS scheme leads to improved ID and EH performance of around 10% compared to conventional PS schemes.

Index Terms—Fluid antenna, SWIPT, SIC, port selection, stochastic geometry.

I. INTRODUCTION

The advent of sixth-generation (6G) networks and the massive Internet of Things (mIoT) concept has led to an increasing demand for sustainable energy supply and ultra-reliable connectivity [1]. To meet this demand, next-generation cellular networks will have to foster beneficial synergies among several innovative technologies, such as simultaneous wireless information and power transfer (SWIPT) technology, successive interference cancellation (SIC), and fluid-based reconfigurable antennas (FAs). FAs refer to liquid radiating elements (e.g., eutectic gallium indium (EGaIn), etc.) that are contained in a dielectric holder and can be programmably and controllably flowed to different locations (ports) within the topological boundaries of the holder. Thus, FAs are capable to reversibly re-configure their physical configuration (i.e., size, shape and feeding) as well as their electrical properties (i.e., resonant frequency, bandwidth), providing a new degree of freedom in the design of wireless communication systems [2].

Owing to the unprecedented benefits offered by FAs, FA-enabled communications have attracted significant interest from both the research community and industry, resulting in their investigation across a diverse range of communication

scenarios. Initially, a contemporary FA-related survey can be found in [2], highlighting the wide range of functionalities attained by the employment of reconfigurable FAs. The achieved outage and ergodic capacity performance of FA-enabled point-to-point communication systems are investigated in [3], as well as in the context of multi-user communication scenario [4]. In particular, the authors illustrate that the performance achieved by an FA-enabled communication system outperforms conventional maximal ratio combining (MRC), if the number of ports is sufficiently large. The beneficial combination of FA technology and full-duplex radio is investigated in [6], where the spatial diversity offered by the FA concept is exploited towards handling the overall interference. Finally, the impact of imperfect channel estimation on the achieved performance of large-scale FA-enabled communication systems is assessed in [7], revealing a trade-off imposed between improving the network's outage performance and reducing the channel estimation quality. Nevertheless, the above studies only focus on enhancing the information decoding (ID) performance of the considered network deployments through the employment of port selection (PS) schemes that ensure the highest received signal strength or the mitigation of the observed interference.

Another critical challenge of next-generation networks is to achieve energy self-sustainability of mIoT devices/applications. This was the key motivating factor for introducing the concept of SWIPT, where UEs are able to extract both information and energy from radio-frequency (RF) signals, thereby prolonging the lifetime of communication networks. The key idea of SWIPT is to split the received RF signal into two distinct parts: one for ID and another for energy harvesting (EH). This can be accomplished in the time, power, or space domain [8]. Throughout the literature, the potential benefits of SWIPT have been widely studied [9]–[11]. Recent works show that the performance of SWIPT, in a large-scale network, is highly affected by the multi-user interference which induces a strong trade-off between ID and EH; that is, high levels of interference increase the harvested energy but deteriorate the performance of ID and vice-versa [10], [11]. Therefore, in order to deal with the counterposed effects introduced by the multi-user interference in large-scale FA-enabled SWIPT networks, sophisticated PS mechanisms that enhance both ID and EH objectives via exploiting the additional degree of freedom offered by the FA technology are required. Nevertheless, to the best of our knowledge, such mechanisms are missing from the current literature.

This work received funding from the European Research Council (ERC) under the European Union's Horizon 2020 research and innovation programme (Grant agreement No. 819819). It was also funded by the European Union's Horizon Europe programme (ERC, WAVE, Grant agreement No. 101112697), and from the LARISSA-6G project under the Cohesion Policy Funds "THALEIA 2021-2027" with EU co-funding.

In this paper, we study the ID and EH outage performance of large-scale FA-enabled SWIPT networks with SIC capabilities. The main contribution of this paper is the development of a novel PS scheme, where the port with the minimum signal-to-interference ratio (SIR) is selected at each UE. The proposed PS scheme utilizes the additional degrees of freedom provided by the FA technology to facilitate the successful SIC implementation, thereby removing the dominant interfering BS and significantly enhancing both ID and EH outage performance. By using stochastic geometry (SG) tools, we analytically derive the ID and the EH outage probabilities, and the performance of the considered system is evaluated under different network parameters. Numerical results demonstrate that, compared to the conventional maximum SIR-based PS, the proposed PS scheme significantly enhances both the ID and EH performance of large-scale FA-enabled SWIPT networks.

II. SYSTEM MODEL

A. Network topology

We consider a downlink cellular network consisting of randomly deployed base stations (BSs), where their locations are modeled as points of a homogeneous Poisson point process (PPP), denoted as $\Phi = \{x_j \in \mathbb{R}^2, j \in \mathbb{N}^+\}$ with spatial density λ_b BS/m². To simplify the notation, we use x_j to present the locations of BSs which are ordered by the distances to the origin. Thus, x_j represents the j -th closest BS to their origin with distance that is denoted as ρ_j . Furthermore, the locations of the UEs follow an arbitrary independent point process Ψ with spatial density $\lambda_u \gg \lambda_b$. Since multiple UEs can exist in the coverage area of a BS, a scheduling technique is employed, which schedules all UEs for their communication with the assigned BS at different time-frequency resources. That means no intra-cell interference exists since intra-cell users are served with orthogonal time-frequency resources. Moreover, we assume that all BSs are equipped with a single omnidirectional antenna, while all UEs are equipped with a single FA (see Section II-B). Without loss of generality and by following Slivnyak's theorem [12], the analysis concerns the typical UE located at the origin but the results hold for all UEs of the network.

B. Fluid antenna model

Fig. 1 illustrates the considered architecture of a fluid-based reconfigurable antenna, which consists of a tube-like linear capillary filled with an electrolyte and a drop of liquid metal that can move freely within the capillary. The antenna's location, which corresponds to the position of the fluid metal, can be promptly switched to one of N preset locations (also known as "ports"). These ports are evenly distributed along the linear dimension of the antenna, which is given by $\kappa\lambda$, where λ is the communication wavelength, and κ is a scaling constant. Fig. 1 also depicts the distance between the first port, that is considered as the reference port, and the i -th port, which is equal to $d_i = \left(\frac{i-1}{N-1}\right)\kappa\lambda$, $\forall i \in \mathcal{N}$, where $\mathcal{N} = \{1, 2, \dots, N\}$. Based on the above, the distance of the

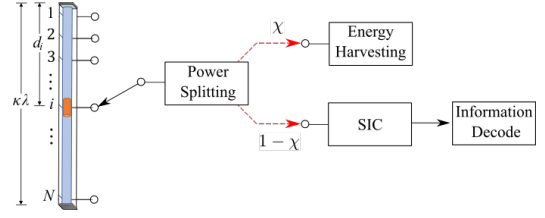


Fig. 1: The considered SWIPT-enabled FA architecture. link between the i -th port of the typical UE and the BS at $x_j \in \mathbb{R}^2$, is given by

$$r_{i,j} = \sqrt{\rho_j^2 + \kappa^2 \lambda^2 \left(\frac{i-1}{N-1}\right)^2}, \quad \forall i \in \mathcal{N}, \quad (1)$$

where ρ_j is the distance between the i -th port of the typical UE and the j -th closest BS, with probability density function (pdf) that is given by [12]

$$f_{\rho_j}(r) = \frac{2(\pi\lambda_b)^{j+1}}{j!} r^{2j+1} \exp(-\pi\lambda_b r^2). \quad (2)$$

C. Channel model

Due to the ultra-dense deployment of BSs, the considered network deployment operates in the interference-limited region i.e., thermal noise is neglected. In addition, we assume that all signals are subject to large-scale path-loss effects. More specifically, a general power-law model is considered in which the signal power decays at the rate r^{-a} with the propagation distance r between a transmitter and a receiver, where a is the path-loss exponent i.e., $\ell(r) = r^{-a}$. Moreover, we assume that all links undergo small-scale fading, which is characterized by the Rayleigh fading model. Due to the ability of FA's ports to be arbitrarily close to each other, their channels are assumed to be correlated. Hence, the channel between the i -th port of the typical UE and a BS at $x_j \in \mathbb{R}^2$, is given by

$g_{x_j}^{(i)}$

$$= \begin{cases} \sigma\alpha_1 + j\sigma\beta_1 & \text{if } i = 1, \\ \sigma\left(\sqrt{1-\mu_i^2}\alpha_i + \mu_i\alpha_0\right) + j\sigma\left(\sqrt{1-\mu_i^2}\beta_i + \mu_i\beta_0\right) & \text{otherwise,} \end{cases}$$

where $\alpha_1, \dots, \alpha_N$ and β_1, \dots, β_N are all independent Gaussian random variables with zero mean and variance of $\frac{1}{2}$ i.e., $\alpha_i, \beta_i \sim \mathcal{N}(0, 1/2)$, and μ_i represents the channel correlation between the i -th port and the reference (i.e., first) port. The appropriate selection of this parameter is crucial for accurately characterizing the correlation behavior of the channel. In our work, we consider $\mu_i = 0$ if $i = 1$, otherwise $\mu_i = J_0\left(\frac{2\pi(i-1)}{N-1}\kappa\right)$ [3]. The joint pdf and cumulative distribution function (cdf) of $|g_{x_1}^{(1)}|, \dots, |g_{x_1}^{(N)}|$, conditioned on ρ_1 , are given by [4]

$$\begin{aligned} & f_{|g_{x_1}^{(1)}|, \dots, |g_{x_1}^{(N)}|}(\tau_1, \dots, \tau_N | \rho_1) \\ &= \prod_{\substack{i \in \mathcal{N} \\ (\mu_i \triangleq 0)}} \frac{2\tau_i}{\sigma^2(1-\mu_i^2)} \exp\left(-\frac{\tau_i^2 + \mu_i^2 \tau_1^2}{\sigma^2(1-\mu_i^2)}\right) I_0\left(\frac{2\mu_i \tau_1 \tau_i}{\sigma^2(1-\mu_i^2)}\right), \quad (3) \end{aligned}$$

and

$$\begin{aligned} & F_{|g_{x_1}^{(1)}|, \dots, |g_{x_1}^{(N)}|}(\tau_1, \dots, \tau_N | \rho_1) \\ &= \int_0^{\tau_1^2} \exp(-y) \prod_{k=2}^N Q_1\left(\sqrt{\frac{2\mu_k^2 y}{(1-\mu_k^2)}}, \sqrt{\frac{2\tau_k}{\sigma^2(1-\mu_k^2)}}\right) dy \quad (4) \end{aligned}$$

respectively, where $\tau_1, \dots, \tau_N \geq 0$, $I_0(\cdot)$ depicts the zero-order modified Bessel function of the first kind and $Q_1(\cdot, \cdot)$ is the first-order Marcum Q-function.

D. Joint wireless information and power transfer model

All BSs are assumed to have a continuous power supply and transmit with power P (dBm). In contrast, all UEs are assumed to be battery-less and capable of simultaneously decoding information and harvesting energy through a power-splitting SWIPT technique, which is depicted in Fig. 1. Specifically, the received power is divided into two parts with a splitting ratio $\chi \in [0, 1]$, where a fraction $(1 - \chi)$ of the received power is consumed for the ID purpose, while the remaining power is driven to the EH circuit [11].

Regarding the EH process, a UE harvests energy from the aggregate RF signal transmitted by all BSs (i.e., tagged and interfering BSs). A practical EH model is adopted, which captures the randomness in the detection of the actual harvested energy [11]. More specifically, the harvested energy of a UE at the i -th port is quantified as following [11]

$$\psi_i = \frac{\chi \nu \eta}{1 + F} \sum_{x_j \in \Phi} P |g_{x_j}^{(i)}|^2 \ell(r_{i,j}), \quad (5)$$

where F is an exponential random variable with mean ζ , $\nu = \zeta e^\zeta \int_{-\zeta}^{\infty} e^{-t}/t dt$, and η is a constant representing the energy conversion efficiency from RF to direct current power.

For the ID process, we adopt the nearest-BS association rule¹ i.e., the typical UE communicates with its closest BS located at $x_1 \in \mathbb{R}^2$. In particular, we assume that each UE employs a SIC technique on the received signal to enhance ID in accordance to [13]. The key idea of SIC is to decode the dominant interference signals and subtract them from the received signal, resulting in an increase of the observed SINR. In order to keep both the computational complexity and power consumption at low levels, we assume that SIC deals only with the dominant interfering BS.

E. Interference Model

The concurrent communication links between the BSs and their associated UEs induce multi-user interference. More specifically, the aggregate multi-user interference observed at the i -th port of the typical UE is given by

$$I_i = \sum_{x_j \in \Phi \setminus x_1} P |g_{x_j}^{(i)}|^2 \ell(r_{i,j}), \quad (6)$$

where $r_{i,j}$ depicts the distance between the i -th port of the typical UE and the j -th closest BS, that is given by (1). Note that the closer interfering BS has the higher impact on the system performance compared to the rest of the interferers. Hence, by aiming the analytical tractability of the developed mathematical framework, we approximate the aggregate network interference by considering the nearest interfering BS and the conditional expectation of the sum of the remaining

interfering BSs [14]. More specifically, the aggregate multi-user interference at the i -th port of the typical UE can be approximated as follows

$$I_i \simeq P |g_{x_2}^{(i)}|^2 \ell(r_{i,j}) + \mathbb{E} \left[\sum_{x_j \in \Phi \setminus \{x_1, x_2\}} P |g_{x_j}^{(i)}|^2 \ell(r_{i,j}) \mid \rho_2 \right]. \quad (7)$$

Let \mathfrak{I}_i represents the average interference from the remaining interferers i.e., $\mathfrak{I}_i = \mathbb{E} \left[\sum_{x_j \in \Phi \setminus \{x_1, x_2\}} P |g_{x_j}^{(i)}|^2 \ell(r_{i,j}) \mid \rho_k \right]$. By using Campbell's theorem and since all fading gains are independent and exponentially distributed with unit mean, \mathfrak{I}_i is given by [12]

$$\mathfrak{I}_i = \frac{2\pi\lambda_b}{a-2} P \ell(r_{i,2})^2. \quad (8)$$

III. FA-ENABLED SWIPT SYSTEMS WITH SIC CAPABILITIES

We assess the overall system performance in terms of EH and ID performance. Initially, we introduce the proposed minimum SIR-based (min-SIR) PS scheme that has been employed. Then, the analytical expressions for the ID and the EH outage probabilities are derived, by using SG tools.

A. Port selection scheme

For a BS to communicate with its associated UE, it is required to adopt a PS scheme in order to determine the location of the FA. We assume that the FA's location of each UE is switched to the port that provides the minimum ratio $|g_{x_1}^{(i)}|/|g_{x_2}^{(i)}|$. The adopted min-SIR PS scheme ensures that the strongest possible overall received signal strength is achieved, resulting in a maximum EH efficiency. Furthermore, the adopted scheme enables the presence of a dominant interfering BS, facilitating the successful implementation of the SIC procedure, and thus leading to an enhanced ID performance. In particular, the proposed scheme exploits the additional degrees of freedom offered by the FA technology via selecting a port that ensures the successful SIC operation, thereby both ID and EH performance can be significantly enhanced. Hence, the FA's location is instantly switched to the port that satisfies²

$$\mathbf{i} = \arg \min_{i \in \mathcal{N}} \left\{ \frac{|g_{x_1}^{(i)}|}{|g_{x_2}^{(i)}|} \right\}. \quad (9)$$

Existing PS schemes, denoted as "max-SIR PS schemes", select the FA port in which the multi-user interference is in deep fade for maximizing the observed SIR, leading to the highest received performance. However, the absence of strong multi-user interference results in a significantly lower overall received signal strength and in the inability of UEs to decode and remove the strongest interfering signal, compromising both EH and ID performance.

²Channel state information (CSI) knowledge can be acquired through various channel estimation techniques, including the utilization of pilot-training symbols or the implementation of advanced vector-based channel estimation techniques. Owing to the strong spatial correlation between the FAs' ports that leads to the requirement of a small number of observed ports/training to achieve full CSI, the overhead induced by the adopted channel estimation technique is omitted.

¹The adopted distance-based association policy requires an a priori knowledge of the location of the BSs. This knowledge can be obtained by monitoring the location of the BSs through a low-rate feedback channel or by a global positioning system mechanism.

$$\Pi^{\text{EH}}(\theta|\rho_1) = \int_0^\infty \frac{2t_1}{\sigma^2} \exp\left(-\frac{t_1^2}{\sigma^2}\right) \left\{ \int_{\frac{\Omega_1 t_1^2}{\sigma^2}}^\infty \exp(-y) \prod_{k=2}^N \left\{ \frac{\Omega_k}{\Omega_k + 1} \exp\left(-\frac{\mu_k^2 \left(\frac{\Omega_k y^2}{\sigma^2} + y\right)}{Z_k(\Omega_k)}\right) I_0\left(\frac{2\mu_k^2 t_1 \sqrt{y\Omega_k}}{\sigma^2 Z_k(\Omega_k)}\right) - Q_1\left(\sqrt{\frac{2\mu_k^2 y}{Z_k(\Omega_k)}}, \tau_1 \sqrt{\frac{2\Omega_k \mu_k^2}{Z_k(\Omega_k)}}\right) \right\} dy \right\} dt_1 \quad (11)$$

$$\Pi^{\text{ID}}(\vartheta, n|\rho_1) = \int_0^\infty \frac{2t_1}{\sigma^2} \exp\left(-\frac{t_1^2}{\sigma^2}\right) \left\{ \int_{\frac{\Upsilon_1 t_1^2}{\sigma^2}}^\infty \exp(-y) \prod_{k=2}^N \left\{ \frac{\Upsilon_k}{\Upsilon_k + 1} \exp\left(-\frac{\mu_k^2 \left(\frac{\Upsilon_k y^2}{\sigma^2} + y\right)}{Z_k(\Upsilon_k)}\right) I_0\left(\frac{2\mu_k^2 t_1 \sqrt{y\Upsilon_k}}{\sigma^2 Z_k(\Upsilon_k)}\right) - Q_1\left(\sqrt{\frac{2\mu_k^2 y}{Z_k(\Upsilon_k)}}, \tau_1 \sqrt{\frac{2\Upsilon_k \mu_k^2}{Z_k(\Upsilon_k)}}\right) \right\} dy \right\} dt_1 \quad (14)$$

B. Energy harvesting performance

We investigate the EH performance, that is mathematically defined as the probability that the instantaneous harvested energy, denoted as ψ_1 , is smaller than a predefined threshold θ , and is expressed as $\Pi^{\text{EH}}(\theta) = \mathbb{P}[\psi_1 \geq \theta]$. This metric provides valuable insights into the effectiveness of an EH-enabled system, as it enables us to quantify the probability that a given level of energy can be reliably harvested. An analytical expression for the EH outage probability is provided in the following theorem.

Theorem 1. *The EH outage probability of the typical UE is given by*

$$\Pi^{\text{EH}}(\theta) = \int_0^\infty \Pi^e(\theta|r) f_{\rho_1}(r) dr, \quad (10)$$

where $\Pi^{\text{EH}}(\theta|r)$ is the conditional EH outage probability, that is given by (11), $f_{\rho_1}(r)$ is the pdf of the distance between the i -th port of the typical UE and its serving BS, that is given by (3), $\Omega_i = r_{i,1}^a \left(\frac{\theta(1+F)}{\chi\nu\eta P} - \frac{\gamma_i}{P} \right)$, and $Z_k(\alpha) = (\alpha + 1)(1 - \mu_k^2)$.

Proof. See Appendix A. \square

C. Information transfer performance

The achieved performance of the considered network deployment in terms of ID outage probability is evaluated, by exploiting the ability of the UEs to perform SIC. In particular, each UE initially attempts to decode the received signal without any interference cancellation. If this attempt is unsuccessful, the UE seeks to decode the dominant interfering signal, subtract it from the received signal, and then re-attempt to decode the resulting received signal³. If the UE is still not able to decode the received signal, then the UE is considered to be in outage. Therefore, the transmission to the i -th port of the typical UE is successful as long as one of the following events is successful

$$\begin{aligned} &0 : (\gamma_i(0) \geq \vartheta) \\ &1 : (\gamma_i(0) < \vartheta) \cap \left(\frac{|g_{x_2}^{(i)}|^2 \ell(r_{i,2})}{\sum_{x_j \in \Phi \setminus \{x_1, x_2\}} |g_{x_j}^{(i)}|^2 \ell(r_{i,j})} \geq \vartheta \right) \cap (\gamma_i(1) \geq \vartheta), \end{aligned} \quad (12)$$

³We assume that the order statistics of the received interfering signal power do not depend on the fading and are determined by the distances [13].

where $\gamma_i(0)$ and $\gamma_i(1)$ are the signal-to-interference ratio (SIR) observed at the i -th port of the typical UE, prior and after the cancellation of the strongest interfering BS. In (12), the first term represents the probability of experiencing an outage while decoding the received signal, and the second term depicts the probability of successfully canceling the strongest interfering signal. Finally, the third term represents the probability of successfully decoding the received signal after canceling the strongest interfering signal.

Initially, let us define the conditional probability of unsuccessfully decoding the desired signal by the selected port of the typical UE, prior and after cancelling the strongest interfering BS i.e., $\Pi_i^{\text{ID}}(\vartheta, n|\rho_1) = \mathbb{P}[\gamma_i(n) < \vartheta|\rho_1]$ with $n \in \{0, 1\}$. Given whether the dominant interferer is successfully canceled or not, the instantaneous outage probability can be defined as in the following Lemma.

Lemma 1. *The outage performance after the successful cancellation of the n strongest interferers is given by*

$$\Pi_i^{\text{ID}}(\vartheta, n) = \int_0^\infty \Pi^{\text{ID}}(\theta, n|r) f_{\rho_1}(r) dr, \quad (13)$$

where $n \in \{0, 1\}$, $\Pi^{\text{ID}}(\theta|r)$ represents the conditional ID coverage probability, that is given by (14), $f_{\rho_1}(r)$ is given by (3), $Z_k(\alpha) = (\alpha + 1)(1 - \mu_k^2)$, and

$$\Upsilon_i = \begin{cases} \frac{\vartheta I_i}{\ell(r_{i,0})} & \text{if } n = 0, \\ \frac{\vartheta \gamma_i}{\ell(r_{i,0})} & \text{if } n = 1. \end{cases}$$

Proof. See Appendix B. \square

Finally, the probability of the UEs to successfully decode and cancel the strongest interfering BS, can be expressed as [13, Lemma 3]

$$\Pi^{\text{D}}(\vartheta) = \left(1 + \vartheta^{\frac{2}{\alpha}} C\left(\frac{1}{\vartheta^{\frac{2}{\alpha}}}, a\right) \right)^{-1},$$

where $C(\alpha, \beta) = \int_\alpha^\infty (1 + w^{\frac{\alpha}{2}})^{-1} dw$. Hence, based on the sequence of events in (12), the following theorem provides the overall outage performance.

Theorem 2. *The ID outage performance for a UE with the ability to perform SIC to cancel the strongest interfering BS, is given by,*

$$\Pi^{\text{ID}}(\vartheta) = \Pi^{\text{ID}}(\vartheta, 0) - \Pi^{\text{ID}}(\vartheta, 0) \Pi^{\text{D}}(\vartheta) (1 - \Pi^{\text{ID}}(\vartheta, 1)). \quad (15)$$

Proof. Since the success of SIC occurs as one of the steps described in (12), the proof follows directly from the definition

of the sequence of events and the use of $\Pi^{\text{ID}}(\vartheta, n)$ and $\Pi^{\text{D}}(\vartheta)$. \square

Note that, the second term of (15) represents the additional achieved gains on the network performance, by exploiting the ability of the UEs to perform SIC. Thus, the ID outage performance achieved by FA-enabled SWIPT networks without SIC capabilities is equal to $\Pi^{\text{ID}}(\vartheta, 0)$.

IV. NUMERICAL RESULTS

In this section, numerical results are provided to verify our model as well as to illustrate the performance of FA-based UEs in large-scale SWIPT cellular networks. Specifically, we consider the following parameters: $\lambda_b = 15\text{BS/km}^2$, $\lambda_u = 30\text{BS/km}^2$, $\lambda = 6\text{ cm}$, $a = 4$, $W = 500\text{ kHz}$, $\sigma = 1$, and $\kappa = 0.2$. Note that, by using different values will lead to a shifted network performance, but with the same conclusions.

Fig. 2 shows the information transfer performance of a FA-enabled large-scale SWIPT cellular network with SIC capabilities in the context of the proposed min-SIR PS scheme versus the threshold ϑ (dB), for different number of FAs' ports $N = \{5, 30\}$. We can easily observe that, the ID outage probability decreases with the increase of the number of FA ports. This was expected, since by increasing the number of FA ports, the spatial diversity also increases, leading to improved SIR observed by the UEs. For comparison purposes, the ID performance achieved by the considered network deployments without SIC capabilities is also displayed in the figure. As expected, by decoding and removing the strongest interfering signal, the UEs face a noticeable weaker interference resulting in an improvement in the observed SIR. Furthermore, Fig. 2 highlights that the performance achieved with the employment of the min-SIR PS scheme can outperform that achieved with the conventional maximum SIR-based PS scheme, denoted as "max-SIR PS scheme" [4]. In particular, the proposed scheme reduces the ID outage performance by around 10% compared with the conventional PS scheme, for the scenario where all FAs are equipped with $N = 30$ ports and threshold $\vartheta = 7$ dB. This again is expected, since the proposed PS scheme ensures the presence of a dominant interfering BS, facilitating the successful cancellation of its induced interfering signal through SIC. In contrast, with the employment of the max-SIR PS scheme, a port with low multi-user interference is selected, thereby UEs' become incapable of decoding and removing the dominant interfering signal. Finally, the agreement between the theoretical curves (solid and dashed lines) and the simulation results (markers) validates our analysis.

Fig. 3 illustrates the energy harvesting performance with respect to the number of FAs' ports N , for different power splitting ratios $\chi = \{0.25, 0.5, 0.75\}$. Similar with the ID performance, the number of FA ports has a negative effect on the EH outage performance. This was expected since, the increased number of FAs' ports results in a higher spatial diversity, and consequently, to a greater overall received signal strength. Another important observation is that, at low number of FA ports, the conventional PS scheme provides slightly

better EH network performance compared to the min-SIR PS scheme. However, by increasing the number of FA ports beyond a critical point, our proposed scheme overcomes the conventional scheme, providing a significantly enhanced EH performance. In particular, for the scenario where all FAs are equipped with larger than $N = 27$ ports and $\chi = 0.75$, the proposed scheme provides an increase of the EH performance by around 10% compared with the conventional PS scheme. Finally, it is obvious that by allocating a larger fraction of received power for EH leads to an improved average RF harvested energy, and thus, to an enhanced EH performance.

V. CONCLUSION

In this paper, we proposed an analytical framework based on SG to study the ID and EH performance of FA-enabled SWIPT networks with SIC capabilities in the context of a novel PS scheme. The proposed scheme leverages the additional degree of freedom offered by the FA technology toward selecting the port that facilitates the cancellation of the dominant interfering BS, thereby leading to enhanced ID and EH performance. Both the ID and EH outage performance were analytically derived and the impact of SIC, power splitting ratio, and number of FAs' ports has been discussed. Our results demonstrated that the proposed min-SIR PS scheme provides significant performance gains compared to conventional solutions in terms of both ID and EH outage probability. A future extension of this work is the consideration of channel models that accurately capture the correlation between FA ports, as well as the investigation of FA technology in the context of SWIPT multiple-input multiple-output systems.

APPENDIX A PROOF OF THEOREM 1

Based on the definition of the EH outage probability,

$$\begin{aligned} \Pi^{\text{EH}}(\theta|\rho_1) &= \mathbb{P} \left[\frac{\chi\nu\eta}{1+F} \sum_{x_j \in \Phi} P|g_{x_j}^{(i)}|^2 \ell(r_{i,j}) < \theta | \rho_1 \right] \\ &\stackrel{(a)}{=} \mathbb{P} \left[\frac{\chi\nu\eta}{1+F} \left(P|g_{x_1}^{(i)}|^2 \ell(r_{i,1}) + I_i \right) < \theta | \rho_1 \right] \\ &= \mathbb{P} \left[P|g_{x_2}^{(i)}|^2 \left(\frac{|g_{x_1}^{(i)}|^2 \ell(r_{i,1})}{|g_{x_1}^{(i)}|^2} + \ell(r_{i,2}) \right) < \frac{\theta(1+F)}{\chi\nu\eta} - \mathcal{I}_i | \rho_1 \right] \\ &\stackrel{(b)}{=} \mathbb{P} \left[\frac{|g_{x_1}^{(i)}|^2}{|g_{x_2}^{(i)}|^2} < \frac{\theta(1+F)}{\chi\nu\eta P \ell(r_{i,1})} - \frac{\mathcal{I}_i}{P \ell(r_{i,1})} - \frac{\ell(r_{i,2})}{\ell(r_{i,1})} | \rho_1 \right], \end{aligned}$$

where $s = \frac{\theta(1+F)}{\chi\nu\eta}$, (a) is derive with the use of the adopted approximation for the aggregate interference, and (b) follows by assuming that the channel of the dominant interfering BS is approximated by its mean value i.e., $|g_{x_2}^{(i)}|^2 \approx \mathbb{E} \left[|g_{x_2}^{(i)}|^2 \right] = 1$. In addition, since $\rho_1 < \rho_2$, and thus $\ell(r_{i,1}) \gg \ell(r_{i,2})$, the term $\frac{\ell(r_{i,2})}{\ell(r_{i,1})}$ is approximately equal to zero, i.e. $\frac{\ell(r_{i,2})}{\ell(r_{i,1})} \rightarrow 0$. Thus, the EH outage probability is given by

$$\Pi^{\text{EH}}(\theta|\rho_1) = \mathbb{P} \left[\frac{|g_{x_1}^{(i)}|^2}{|g_{x_2}^{(i)}|^2} < r_{i,1}^a \left(\frac{\theta(1+F)}{\chi\nu\eta P} - \frac{\mathcal{I}_i}{P} \right) | \rho_1 \right].$$

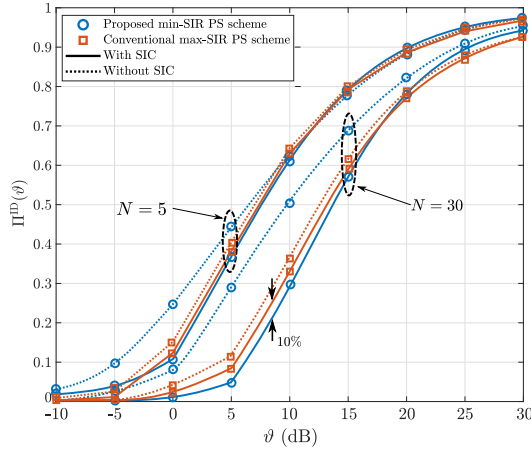


Fig. 2: ID outage performance versus the threshold ϑ (dB) for different number of ports N .

Let $\Omega_i = r_{i,1}^a \left(\frac{\theta(1+F)}{\chi\nu\eta P} - \frac{\mathcal{I}_i}{P} \right)$. Based on the adopted port selection scheme, $\Pi^{\text{EH}}(\theta\rho_1)$ can be expressed as

$$\begin{aligned} \Pi^{\text{EH}}(\theta|\rho_1) &= \mathbb{P} \left[\min_{i \in \mathcal{N}} \left\{ \frac{|g_{x_1}^{(i)}|}{|g_{x_2}^{(i)}|} \right\} < \sqrt{\Omega_i} |\rho_1| \right] \\ &= 1 - \mathbb{P} \left[|g_{x_1}^{(1)}| > \sqrt{\Omega_1} |g_{x_2}^{(1)}|, \dots, |g_{x_1}^{(N)}| > \sqrt{\Omega_N} |g_{x_2}^{(N)}| \middle| \rho_1 \right] \\ &= 1 - \int_0^\infty \dots \int_0^\infty \mathbb{P} \left[|g_{x_1}^{(1)}| > \sqrt{\Omega_1} t_1, \dots, |g_{x_1}^{(N)}| > \sqrt{\Omega_N} t_N \middle| \rho_1 \right] \\ &\quad \times f_{|g_{x_2}^{(1)}|, \dots, |g_{x_2}^{(N)}|}(t_1, \dots, t_N | \rho_1) dt_1 \dots dt_N, \end{aligned}$$

where the conditional complementary cdf of $|g_{x_1}^{(1)}|, \dots, |g_{x_1}^{(N)}|$ can be calculated based on (4) i.e., $\mathbb{P} \left[|g_{x_1}^{(1)}| > \sqrt{\Omega_1} t_1, \dots, |g_{x_1}^{(N)}| > \sqrt{\Omega_N} t_N \middle| \rho_1 \right] = 1 - F_{|g_{x_1}^{(1)}|, \dots, |g_{x_1}^{(N)}|}(\tau_1, \dots, \tau_N | \rho_1)$, while the conditional pdf i.e., $f_{|g_{x_2}^{(1)}|, \dots, |g_{x_2}^{(N)}|}(t_1, \dots, t_N | \rho_1)$, is given by (3). Then, the final expression can be achieved by un-conditioning the above expression with the pdf of ρ_1 i.e., $f_{\rho_1}(r)$ that is given by (2), which gives the desired expression.

APPENDIX B PROOF OF LEMMA 1

Based on the definition, $\Pi_1^{\text{ID}}(\vartheta, n | \rho_1)$ is given by

$$\begin{aligned} \Pi_1^{\text{ID}}(\vartheta, n | \rho_1) &= \mathbb{P} \left[\frac{P |g_{x_1}^{(1)}|^2 \ell(r_{i,1})}{\sum_{x_k \in \Phi} \mathbb{1}_{k \geq n+1} I_i(k)} < \vartheta \middle| \rho_1 \right] \\ &\stackrel{(a)}{=} \mathbb{P} \left[\frac{|g_{x_1}^{(1)}|}{|g_{x_2}^{(1)}|} < \sqrt{\frac{\vartheta}{\ell(r_{i,1})} \sum_{x_k \in \Phi} \mathbb{1}_{k \geq n+1} |g_{x_k}^{(i)}|^2 \ell(r_{i,j})} \middle| \rho_1 \right], \end{aligned}$$

where $\mathbb{1}_{k \geq n+1}$ is an indicator function i.e., $\mathbb{1}_A = 1$ if and only if A holds, otherwise $\mathbb{1}_A = 0$. Then, by assuming that $|g_{x_2}^{(i)}|^2 \approx \mathbb{E}[|g_{x_2}^{(i)}|^2] = 1$ and based on the adopted interference model, $\Pi_1^{\text{ID}}(\vartheta, n)$ can be re-written as

$$\Pi_1^{\text{ID}}(\vartheta, n | \rho_1) = \mathbb{P} \left[\min_{i \in \mathcal{N}} \left\{ \frac{|g_{x_1}^{(i)}|}{|g_{x_2}^{(i)}|} \right\} < \sqrt{\Upsilon_i} |\rho_1| \right],$$

where

$$\Upsilon_i = \begin{cases} \frac{\vartheta I_i}{\ell(r_{i,0})} & \text{if } n = 0, \\ \frac{\vartheta \mathcal{I}_i}{\ell(r_{i,0})} & \text{if } n = 1. \end{cases}$$

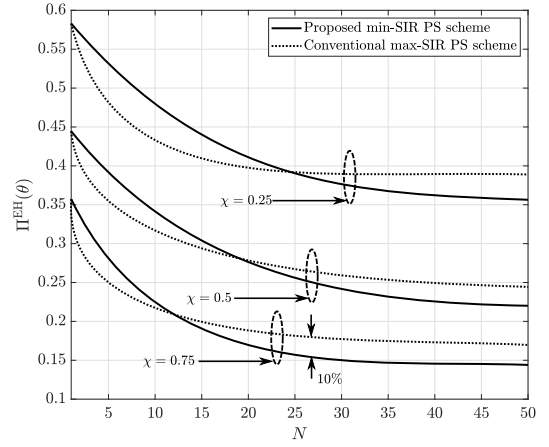


Fig. 3: EH outage performance versus the number of ports N for different values of χ ; $\theta = 0$ dB and $P = 0$ dBm.

Then, by following similar methodology as in Appendix A, we can derive the final expression.

REFERENCES

- [1] I. F. Akyildiz, A. Kak, and S. Nie, "6G and beyond: The future of wireless communications systems," *IEEE Access*, vol. 8, pp. 133995–134030, 2020.
- [2] Y. Huang, L. Xing, C. Song, S. Wang, and F. Elhouni, "Liquid antennas: Past, present and future," *IEEE Open J. Antennas Propag.*, vol. 2, pp. 473–487, 2021.
- [3] K. K. Wong, A. Shojaeifard, K. F. Tong, and Y. Zhang, "Fluid antenna systems," *IEEE Trans. Wireless Commun.*, vol. 20, no. 3, pp. 1950–1962, Mar. 2021.
- [4] K. K. Wong and K. F. Tong, "Fluid antenna multiple access," *IEEE Trans. Wireless Commun.*, vol. 21, no. 7, pp. 4801–4815, Jul. 2022.
- [5] M. Khammassi, A. Kammoun, and M.-S. Alouini, "A new analytical approximation of the fluid antenna system channel," *arXiv preprint arXiv:2203.09318*, 2023.
- [6] C. Skouroumounis and I. Krikidis, "Fluid antenna-aided full duplex communications: A macroscopic point-of-view," *arXiv preprint arXiv:2304.04435*, 2023.
- [7] C. Skouroumounis and I. Krikidis, "Fluid antenna with linear MMSE channel estimation for large-scale cellular networks," *IEEE Trans. Commun.*, vol. 71, no. 2, pp. 1112–1125, Feb. 2023.
- [8] I. Krikidis, S. Timotheou, S. Nikolaou, G. Zheng, D. W. K. Ng, and R. Schober, "Simultaneous wireless information and power transfer in modern communication systems," *IEEE Commun. Mag.*, vol. 52, no. 11, pp. 104–110, Nov. 2014.
- [9] R. Zhang and C. K. Ho, "MIMO broadcasting for simultaneous wireless information and power transfer," *IEEE Trans. Wireless Commun.*, vol. 12, no. 5, pp. 1989–2001, May 2013.
- [10] M. Di Renzo and W. Lu, "System-level analysis and optimization of cellular networks with simultaneous wireless information and power transfer: Stochastic geometry modeling," *IEEE Trans. Veh. Technol.*, vol. 66, no. 3, pp. 2251–2275, Mar. 2017.
- [11] N. Deng and M. Haenggi, "The energy and rate meta distributions in wirelessly powered D2D networks," *IEEE J. Sel. Areas Commun.*, vol. 37, no. 2, pp. 269–282, Sep. 2019.
- [12] M. Haenggi, *Stochastic geometry for wireless networks*, in Cambridge, U.K.: Cambridge Univ. Press, 2012.
- [13] M. Wildemeersch, T. Q. S. Quek, M. Kountouris, A. Rabbachin, and C. H. Slump, "Successive interference cancellation in heterogeneous networks," *IEEE Trans. Commun.*, vol. 62, no. 12, pp. 4440–4453, Dec. 2014.
- [14] Y. Qin, M. A. Kishk, and M.-S. Alouini, "A dominant interferer plus mean field-based approximation for SINR meta distribution in wireless networks," *arXiv preprint arXiv:2302.03574*, 2023.